



ELSEVIER

Polymer 43 (2002) 6911–6929

**polymer**[www.elsevier.com/locate/polymer](http://www.elsevier.com/locate/polymer)

# Rheological study of the influence of $M_w$ and comonomer type on the miscibility of m-LLDPE and LDPE blends

Tayyab Hameed, Ibnelwaleed A. Hussein\*

Department of Chemical Engineering, King Fahd University of Petroleum and Minerals, Dhahran 31261, Saudi Arabia

Received 30 July 2002; received in revised form 7 September 2002; accepted 11 September 2002

## Abstract

The influences of molecular weight and m-LLDPE comonomer type on the miscibility of m-LLDPE with LDPE in the melt state were investigated with rheological methods. Dynamic, steady shear and transient measurements were carried out in an ARES rheometer at 190 °C. The  $M_w$  of the shortly branched m-LLDPE has influenced its miscibility with LDPE and immiscibility has increased with the increase in  $M_w$  of m-LLDPE. The miscibility of the high- $M_w$  m-LLDPE with LDPE was non-symmetric with respect to composition as revealed by the dependence of their  $\eta_0$ ,  $\eta'(\omega)$ ,  $G'$ ,  $N_1(\dot{\gamma})$ , and  $N_1(t)$  on blend composition. Addition of a small amount of the hexene m-LLDPE to LDPE was more likely to cause immiscibility than the addition of a small amount of LDPE to m-LLDPE. Increasing the m-LLDPE branch length (comonomer) from butene to hexene did not influence the miscibility of m-LLDPE/LDPE blends. Agreement was observed between the measured rheology and theoretical predictions of Einstein, Scholz et al., Paliere and Bousmina emulsion models. The ratio of interfacial tension to droplet radius was estimated to be  $\sim 10^3$  N/m<sup>2</sup>. © 2002 Elsevier Science Ltd. All rights reserved.

**Keywords:** Rheology; Polyethylene blend; Miscibility

## 1. Introduction

Despite the fact that miscibility of polyethylene–polyethylene blends has obvious implications on the thermodynamics and on the rheology and final properties, still there are some questions that were not answered to everyone's satisfaction. Blends of linear low density polyethylene (LLDPE) and low density polyethylene (LDPE) find wide use in film applications. Yet, the miscibility of LLDPE and LDPE blends has received far less attention than have linear/branched blends [1–5].

Blends of HDPE/HDPE and LDPE/LDPE (different  $M_w$  fractions) were reported to be miscible [6–9] and the viscosity vs. composition relationship followed the log-additivity rule. Utracki and Schlund [10] found that a blend of LLDPE/LDPE was immiscible; however, other blends of LLDPE/LDPE were reported to be partially miscible [7, 11–15].

Due to the diversity of composition, molecular structure,  $M_w$  and MWD the LLDPE/LDPE blends may or may not be

miscible in specific cases. Hence, blends of LLDPE with other LLDPE or LDPE may show a widely diverse behavior, dependent on small changes in molecular structure caused by, e.g. different catalyst, polymerization method or composition [8]. Most of the previous studies made use of Ziegler–Natta (ZN) LLDPEs.

It should be noted that Ziegler–Natta catalysis produces simultaneously linear and branched chains [16–18]. Further, the details of the molecular structure are becoming more important in view of the reported immiscibility of LLDPE/LLDPE systems and liquid–liquid phase separation in 'pure' LLDPE [19–22]. So, these ZN-LLDPE products were suggested of being intrinsically multiphase even before blending with HDPE or LDPE components. Unfortunately, the use of ZN-LLDPE in miscibility studies renders *inconclusive* results with respect to the effect of molecular parameters, since it is difficult to isolate these parameters.

The effect of molecular weight and branch type was studied for blends of linear and branched polyethylenes. Hill and co-workers [23,24] found no significant effect for varying the  $M_w$  of HDPE ( $2 \times 10^3$ – $2 \times 10^6$ ) on its miscibility with LDPE. However, recent work of Tanem and Stori [4] showed significant effect for  $M_w$  of LLDPE on

\* Corresponding author. Tel.: +1-966-3-860-2235; fax: +1-966-3-860-4234.

E-mail address: ihussein@kfupm.edu.sa (I.A. Hussein).

its miscibility with linear polyethylene (Fig. 10 of Ref. [4]). Both studies used differential scanning calorimetry (DSC) and transmission electron microscopy (TEM) techniques.

Also, the effect of branch type was investigated for blends of linear and branched polyethylenes by DSC, TEM and small angle neutron scattering (SANS) techniques [4, 25,26]. Their results showed that increasing the comonomer from butene to hexene *did not* influence miscibility. However, the effect of  $M_w$  and branch type on the miscibility of m-LLDPE/LDPE blends is yet to be examined and will be the subject of the current study.

Here, rheology will be used to study the effect of  $M_w$  and branch type on the miscibility of m-LLDPE/LDPE blends. Plochocki [27] surveyed the rheology of various kinds of polyolefin blends and Utracki [8] reviewed that of polyethylenes in particular.

For immiscible blend systems, the state of dispersion and specifically the shape of the dispersed phase (i.e. droplets) greatly influence the rheological responses. As illustrated by Chuang and Han [28] rheological behavior of immiscible blends is strongly affected by the type of applied shear. While shear-induced mixing is observed in some steady shear experiments [29,30], no such effects are reported for small amplitude dynamic shear [28,31].

Generally, phase separation causes the storage and loss moduli  $G'$  and  $G''$  to exceed values for the matrix phase, due to the presence of droplets of the dispersed phase. This increase is a result of 'emulsion morphology' present in phase separated systems. Even in a mixture of two Newtonian liquids, the emulsion morphology gives rise to a non-zero  $G'$ . That is, their emulsion exhibits elastic behavior due to surface tension between the phases, in addition to the viscous nature [32,33].

The hydrodynamic calculations [32] for such systems were for dilute emulsions, and an extension to concentrated emulsions (to order  $\phi^2$ ) was given by Choi and Schowalter [34]. They derived expressions for  $G'$  and  $G''$  for an emulsion of two Newtonian liquids, which can also be applied to a phase separated polymeric system in the low- $\omega$  Newtonian regime [35,36], where the  $G'$  had increased due to the presence of droplets. Scholz et al. [35] derived a constitutive equation for dilute emulsions of non-interacting, spherical and monodisperse droplets of Newtonian liquids. The two liquids are assumed to be incompressible, and totally immiscible. For the linear viscoelastic range of deformation, the emulsion was shown to have dynamic moduli given by:

$$\frac{G''(\omega)}{\omega} = \eta' = \eta_m \left[ 1 + \phi \left( \frac{2.5k + 1}{k + 1} \right) \right] \quad (1)$$

$$G'(\omega) = \frac{\eta_m^2 \phi}{80(\alpha/R)} \left( \frac{19k + 16}{k + 1} \right)^2 \omega^2 \quad (2)$$

where  $\eta_m$ , is the viscosity of the matrix liquid;  $\eta_d$ , the viscosity of the dispersed droplets;  $k = \eta_d/\eta_m$ ;  $R$ , the radius

of the dispersed domains;  $\alpha$ , the surface tension between the two liquids;  $\phi$ , the volume fraction of the dispersed phase.

At low  $\omega$ ,  $G'(\omega)$  obtained experimentally for immiscible polymer blends, other than PE/PE systems, was reported to be higher than those of the components [28,35,36–38]. Ajjji and Choplin [39] found that effects of phase separation on  $G'$  were more pronounced than on  $G''$ . Earlier, Martinez and Williams [40] showed similar increase in  $\eta'(\phi)$  and  $\eta'(\dot{\gamma})$  for an immiscible HDPE/PMMA system. Their SEM micrographs supported the rheological measurements.

Scholz et al. [35] reported that the values of the dynamic moduli at high  $\omega$  ( $\omega > 10$  rad/s) for the immiscible blend of PP/Polyamide 6 were intermediate between those of PA6 and PP. Hence, the high- $\omega$  data were *not* used for the interpretation of the miscibility of blends.

In this research project, the rheology of m-LLDPE and LDPE blends is studied. The aim of this investigation is to examine the effects of  $M_w$ , molecular architecture (branch type, branch content) on the miscibility of m-LLDPE blends with LDPE in the melt state. The matrix of resins used as blend components was designed to study one variable at a time. In this first paper, only the effect of  $M_w$  and branch type will be discussed and other parameters will be treated in future publications. Two pairs of m-LLDPE and LDPE were selected to study the effect of  $M_w$ . A high- $M_w$  m-LLDPE and a low- $M_w$  m-LLDPE were blended with the same LDPE. The effect of the m-LLDPE branch type was investigated by comparing blends of a butene-based m-LLDPE and a hexene-based m-LLDPE of the same  $M_w$  and density.

## 2. Experimental

### 2.1. Materials

Three commercial samples of m-LLDPE (two hexene and one butene) and one LDPE were obtained from ExxonMobil. Table 1 provides characterization data such as density at room temperature, melt index (MI) at 190 °C as provided by ExxonMobil. The number-average and weight-average molecular weights as well as polydispersity (PD) were obtained by gel permeation chromatography (GPC). GPC data was collected using 1,2,4 trichlorobenzene as solvent at 150 °C in a WATERS GPC2000 instrument. Polystyrene standards were used for calibration. The label 1 denotes the m-LLDPE with low  $M_w$  as m-EH1 and the resin with high  $M_w$  was labeled m-EH2. Both m-EH1 and m-EH2 were hexene-based, while m-EB is butene based. The same LDPE was used in all of these blends. Blends of 10, 30, 50, 70, and 90% by weight LLDPE were studied. The effect of  $M_w$  of LLDPE was investigated by studying blends of m-EH1 and LDPE and results were compared to those of m-EH2 and LDPE blends. Samples m-EH1 and m-EH2 were chosen in a way that molecular weight would be the *only* molecular parameter in this comparison. As shown in

Table 1  
Characterization of resins

Resin	Density (g/cm <sup>3</sup> )	MI (g/10 min)	$M_w$ (kg/mol)	PD = $M_w/M_n$	Branch content CH <sub>3</sub> /1000 C
m-EH1	0.900	7.5	67	1.85	21.1
m-EH2	0.900	1.2	108	1.83	18.0
m-EB	0.900	1.2	110	1.78	20.4
LDPE	0.923	1.2	100	4.14	7.8 <sup>a</sup>

<sup>a</sup> Total number of short branches.

Table 1, m-EH1 and m-EH2 were of the same branch type (hexene), density (branch content), and both LLDPEs were metallocene resins. Hence, comparison of m-EH1 and m-EH2 blends with LDPE will reveal the effect of  $M_w$  on the miscibility of m-LLDPE/LDPE systems. On the other hand, comparison of m-EH1 and m-EB blends with LDPE will disclose the influence of branch length on the miscibility of LLDPE/LDPE blends.

### 2.2. Melt conditioning in a Haake Polydrive

The LDPE and LLDPE resins used in this study were conditioned (or blended) in a Haake PolyDrive melt blender for 10 min at 50 rpm and 190 °C. Blends of m-EH1, m-EH2, and m-EB with LDPE as well as pure resins were all conditioned in the presence of 1000 ppm of additional antioxidant (AO) to keep the polymer(s) from degradation during melt blending [41]. The AO is a 50/50 blend of Irganox 1010 and Irgafos 168 obtained from Ciba-Geigy. Test for degradation during melt blending was performed for all pure resins. The rheology of as-received resins was compared to the rheology of the same sample conditioned at 190 °C in the presence of extra AO. For example, dynamic viscosity,  $\eta'$ , and elastic modulus,  $G'$ , were obtained as function of frequency,  $\omega$ , for sample m-EH2. Results were shown in Fig. 1(a). Excellent reproducibility of data for conditioned and as-received resin indicates prevention of degradation during melt blending.

### 2.3. Specimen preparation in a Carver press

In all cases, PE samples obtained from melt blender were given a controlled thermomechanical history (molding) before introduction into the rheometer for shear testing. The molding operation, in a Carver press, produced flat discs (25 mm diameter, 2 mm thick) for insertion between the rheometer platens. Molding was conducted at 170 °C after preheating for 4 min. The loaded sample was then placed under 3 ton of pressure for 5 min, followed by an increase to 7 ton for 4 min. After the mold was water-cooled for 10 min, the PE disk was removed at room temperature and inserted between the rheometer platens.

### 2.4. Rheological measurements in ARES

Advanced Rheometrics Expansion System (ARES),

recently acquired through a KFUPM-funded project, was employed for steady-shear, dynamic, and transient measurements. The rheometer is a constant strain rheometer equipped with a heavy transducer (range 2–2000 g) for normal force; 2–2000 g cm for torque. Standard calibration procedures were performed on regular basis. Nitrogen gas (99.99% purity) was continuously used for heating the samples during testing to avoid sample degradation. All tests were carried out using a cone-and-plate set; the cone angle was 0.1 rad, and platen diameter was 25 mm.

With the sample in position, the oven was closed and the polymer heated for 3 min, when the upper platen force transducer assembly was lowered to the proper working position at a constant load of 500 g. The loading procedure was automatically terminated when the cone flattened tip position was separated from the opposing platen by 48  $\mu$ m. Melt extruded beyond the platen rim by this procedure was removed by a razor blade. A holding period of 2–3 min was allowed before beginning measurements when the temperature reaches steady state ( $T = 190 \pm 0.01$  °C). In the case of dynamic testing, a shear strain amplitude ( $\gamma^0$ ) of 15% was used, after a strain sweep showed that this  $\gamma^0$  was sufficiently small to produce dynamic properties in the linear viscoelastic regime. All experiments were performed in a descending- $\omega$  order (from  $10^2$  to  $10^{-2}$  rad/s) and some tests were terminated before the final frequency was reached when the torque signal approaches the sensitivity limit of the transducer. (This was meant to reduce measurement time since collection of data at low- $\omega$  takes longer and the data may not be useful if it were below the sensitivity limits of the rheometer). As suggested earlier by Hussein et al. [41] that a check for degradation and reproducibility of rheological measurements should use samples prepared from different batches. Here, a 50/50 blend of m-EH2 with LDPE was taken as an example. Results for  $\eta'$  and  $G'$  on samples obtained from two different batches were shown in Fig. 1(b). Excellent agreement of data shows the degree of reproducibility of these measurements.

Steady-shear testing was always conducted with a fresh sample. Tests began at the lowest shear rate (usually  $\dot{\gamma} = 0.01$  s<sup>-1</sup>) and continued up to 5 s<sup>-1</sup> to avoid the known hydrodynamic instabilities, when secondary flow causes radial ejection of the sample. In cone-and-plate tests, data on  $\eta(\dot{\gamma})$  and  $N_1(\dot{\gamma})$  were obtained. Steady-shear measurements

were made with unidirectional platen rotation (counterclockwise). The first normal stress difference  $N_1(t)$  was obtained during a step-rate test followed by relaxation. ARES was programmed to perform a  $\dot{\gamma}$ -sweep after allowing 200 s before each measurement, followed by 30 s of measurement time.

### 3. Results and discussion

#### 3.1. Influence of $M_w$

The dynamic and steady-shear measurements were obtained at 190 °C for m-EH1 and m-EH2 blends with LDPE as well as the pure polymers. The blends were characterized primarily by the following rheological functions:  $\eta'$  (or  $G''$ ) and  $\eta''$  (or  $G'$ ) as functions of composition,  $\phi$ , and frequency,  $\omega$ ;  $N_1(\dot{\gamma})$  and  $\phi$ ;  $N_1(t)$  during step rate and relaxation tests.

For blends of m-EH1 ( $M_w = 67k$ ) blends with LDPE data for  $\eta'(\omega)$  and  $G'(\omega)$  were shown in Fig. 2(a) and (b), respectively. Results were shown for the 10, 30, 50, 70, and 90% m-EH1 blends with LDPE as well as for the pure resins. Filled symbols were used for pure polymers, while open symbols represent the different blends. The same symbol was used for the same composition in all the figures. A Newtonian plateau that extended over a period of three decades was observed for the metallocene resin, m-EH1. Also, the m-EH1 resin showed the lowest values for both  $\eta'(\omega)$  and  $G'(\omega)$ . Over a wide range of  $\omega$ , the increase in both  $\eta'$  and  $G'$  for all blends was found to follow the increase in the fraction of the more viscous component. Also, both  $\eta'$  and  $G'$  for all blended component were found to lie between those of the pure resins. The rheology of blends of the low- $M_w$  pair with LDPE suggests the miscibility of the m-EH1 blend with LDPE in the whole composition range.

On the other hand, plots of  $\eta'(\omega)$  and  $G'(\omega)$  for blends of m-EH2, ( $M_w = 108k$ ) with LDPE were given in Fig. 3(a) and (b), respectively. Here, the high- $M_w$  pair showed a Newtonian plateau over more than a decade. Again, the metallocene resin was the component of the lowest viscosity and elasticity over the low- $\omega$  range (0.01–0.1 rad/s). The low- $\omega$  data is especially sensitive to changes in the morphology and hence will be used for the interpretations of the blend miscibility. In the low- $\omega$  range, blends with 50, 30, and 10% m-EH2 (LDPE-rich blends) showed both  $\eta'$  and  $G'$  were higher than those of LDPE. LDPE was the component with the highest viscosity and elasticity. The increase in  $\eta'$  and  $G'$  of LDPE as a result of the addition of a low viscosity component is a clear indication of the presence of multiphase systems and can only be explained by emulsion rheology. These results suggest the immiscibility of the 10, 30, and 50%

m-EH2 blends with LDPE. However, the increase in both  $\eta'$  and  $G'$  for blends of 70 and 90% m-EH2 (m-LLDPE-rich blends) was much less and blends could be totally or partially miscible as will be shown in other plots.

Further, ARES Orchestrator software was used to fit the  $\eta'(\omega)$  data for blends of m-EH1 and m-EH2 with LDPE to the Cross model. Zero shear viscosity,  $\eta_0$ , was obtained from the fitting and results for both pairs were displayed in Fig. 4(a) and (b), respectively. The plot of  $\eta_0(\phi)$ , shown in Fig. 4(a), showed weak positive deviation behavior (PDB) from log-additivity rule suggesting a high degree of miscibility of the low- $M_w$  pair. As shown in Fig. 4(a), the deviations of the low- $M_w$  pair from emulsion rheology are large. The results support the previous findings from  $\eta'(\omega)$  and  $G'(\omega)$  data given in Fig. 2(a) and (b). However,  $\eta_0(\phi)$  for the high- $M_w$  pair was different. Data in Fig. 4(b) showed strong PDB from log-additivity for the 50/50 and the LDPE-rich blends. Hence, these blends are suggested to be immiscible. To determine the degree of immiscibility Einstein model [42] for dilute emulsions of Newtonian fluids [ $\eta_b = \eta_m(1 + 2.5\phi)$ ] was used in this case. Model predictions for the 10% m-EH2 blend, given as a solid line, suggest the complete immiscibility of the 10% blend of m-EH2 with LDPE. On the other side, the 70 and the 90% m-EH2 blends were suggested to be partially miscible with increased degree of miscibility in the m-LLDPE-richer range as predicted from Fig. 4(b).

Data for  $\eta'(\phi)$  at low  $\omega$  near-Newtonian regime ( $\omega = 0.1$  rad/s) were extracted from Figs. 2(a) and 3(a) and plotted in Fig. 4(c) and (d), respectively. Data in Fig. 4(c) suggest the high degree of miscibility of the low- $M_w$  pair and agree with the above findings. For the high- $M_w$  pair, results for  $\eta'(\phi)$  at  $\omega = 0.1$  rad/s (Fig. 4(d)) followed the same pattern of the previous plot of  $\eta_0(\phi)$ , shown in Fig. 4(b). For the 10% blend of m-EH2 with LDPE, the experimental data agree with the predictions of Eq. 1 derived by Scholz et al. model [35]. Plots of  $\eta'(\phi)|_{\tau=\text{const}}$  obtained through curve fitting of  $\eta'(\tau)$  data (suggested by Van Oene [43] since the boundary conditions at the immiscible fluid–fluid interfaces require the continuity of the shear stress,  $\tau$ ) produced similar results that were not shown here. At constant  $\tau$ , plots of  $\eta'(\phi)|_{\tau=\text{const}}$  lead to  $(\partial\eta'/\partial\phi)_\tau > (\partial\eta'/\partial\phi)_\omega$  since  $\{(\partial\eta'/\partial\phi)_\tau = (\partial\eta'/\partial\phi)_\omega \times [1 - \omega(\partial\eta'/\partial\tau)_\phi]\}$  and  $(\partial\eta'/\partial\tau)_\phi$  is negative.

For further examination of the miscibility/immiscibility of the high- $M_w$  pair, data of  $G'(\phi)$  at low  $\omega$  ( $\omega = 0.04$  rad/s) was displayed in Fig. 5(a). Again, immiscibility is strong for the 50/50 and the LDPE-rich blends; the m-LLDPE-rich blends have shown much stronger miscibility. For the 10% m-EH2 blend of the high- $M_w$  pair, Eq. 1 suggests complete immiscibility of the pair (Fig. 4(d)) and hence Eq. 2 was used to calculate the

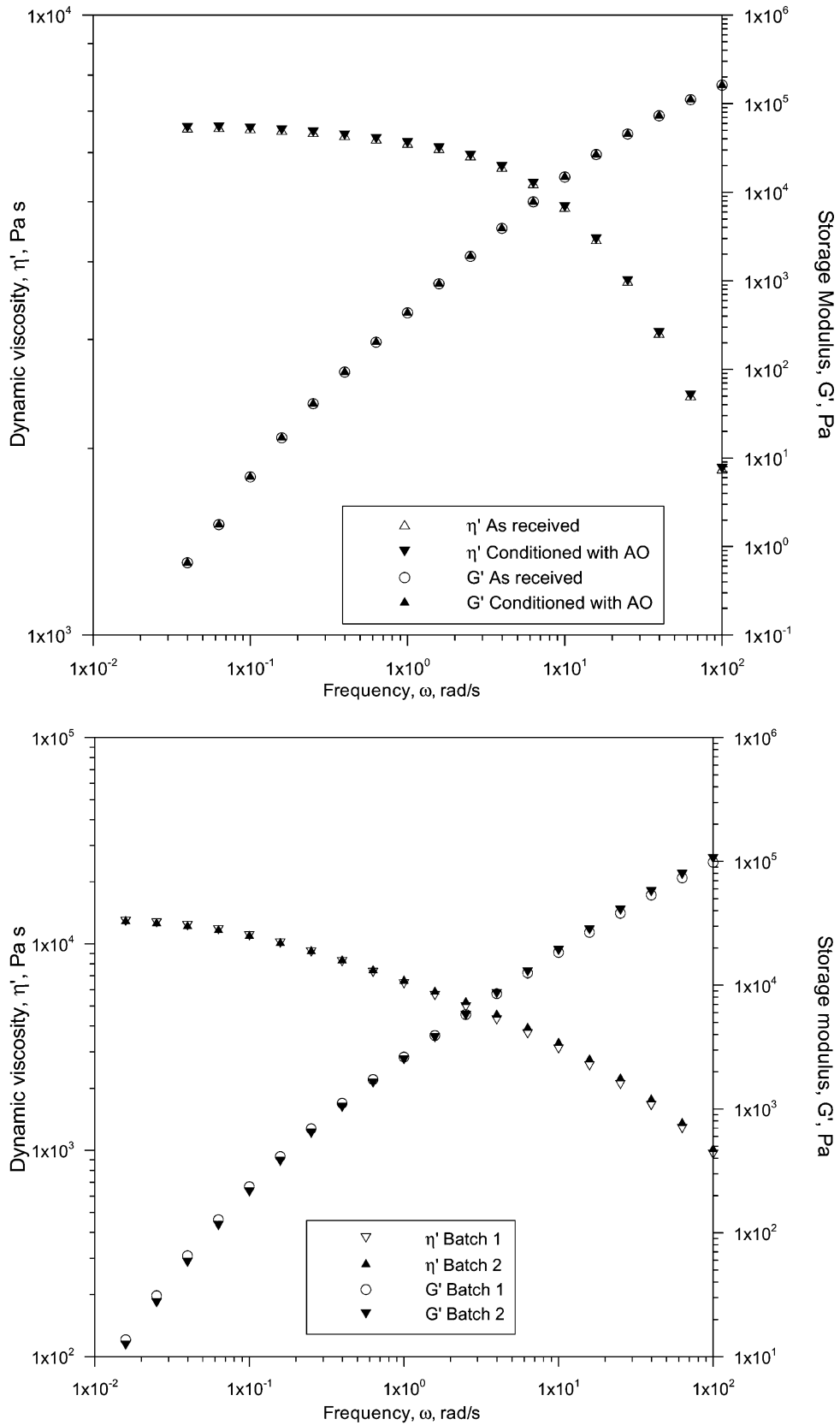


Fig. 1. (a) Comparison of the rheology of as-received and conditioned m-EH2 ( $T_{\text{mix}} = 190^\circ\text{C}$ ,  $T_{\text{test}} = 190^\circ\text{C}$ ,  $\gamma^0 = 15\%$ ). (b)  $\eta'(\omega)$  and  $G'(\omega)$  for 50% m-EH2 blend with LDPE ( $T_{\text{mix}} = 190^\circ\text{C}$ ,  $T_{\text{test}} = 190^\circ\text{C}$ ,  $\gamma^0 = 15\%$ ).

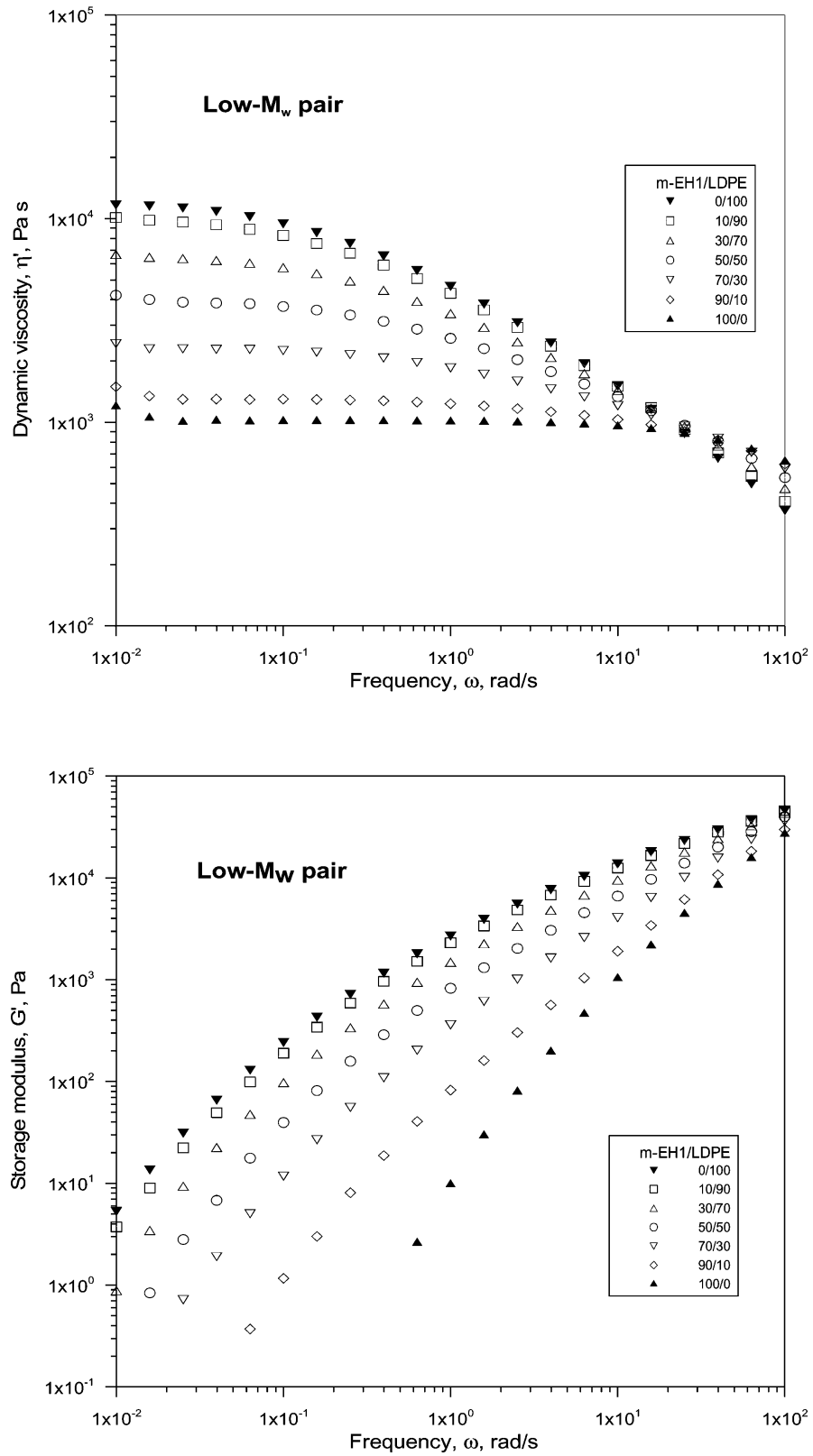


Fig. 2. (a)  $\eta'(\omega)$  for blends of m-EH1 and LDPE ( $T_{\text{mix}} = 190^\circ\text{C}$ ,  $T_{\text{test}} = 190^\circ\text{C}$ ,  $\gamma^0 = 15\%$ ). (b)  $G'(\omega)$  for blends of m-EH1 with LDPE ( $T_{\text{mix}} = 190^\circ\text{C}$ ,  $T_{\text{test}} = 190^\circ\text{C}$ ,  $\gamma^0 = 15\%$ ).

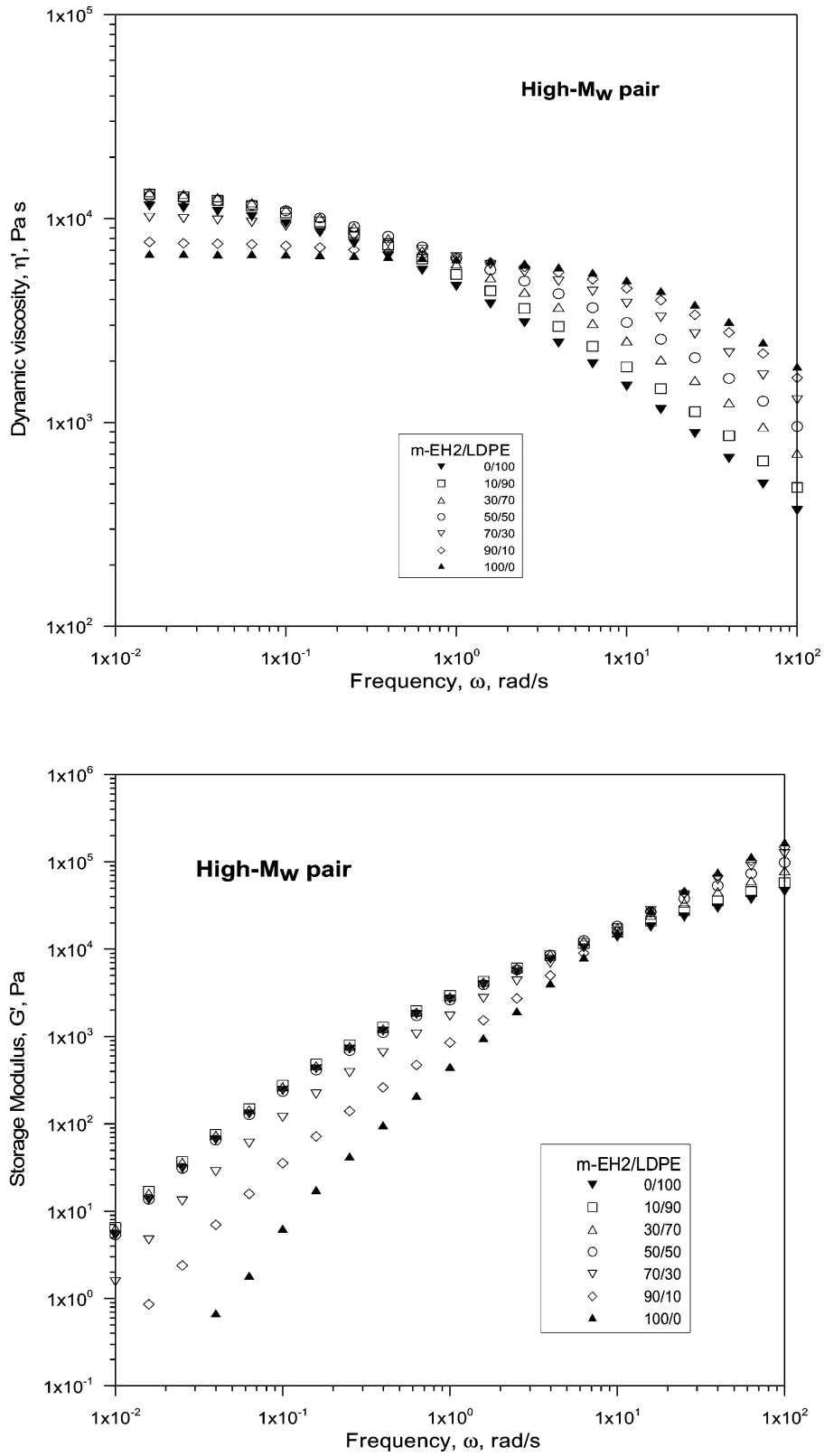


Fig. 3. (a)  $\eta'(\omega)$  for blends of m-EH2 with LDPE ( $T_{\text{mix}} = 190\text{ }^\circ\text{C}$ ,  $T_{\text{test}} = 190\text{ }^\circ\text{C}$ ,  $\gamma^0 = 15\%$ ). (b)  $G'(\omega)$  for blends of m-EH2 with LDPE ( $T_{\text{mix}} = 190\text{ }^\circ\text{C}$ ,  $T_{\text{test}} = 190\text{ }^\circ\text{C}$ ,  $\gamma^0 = 15\%$ ).

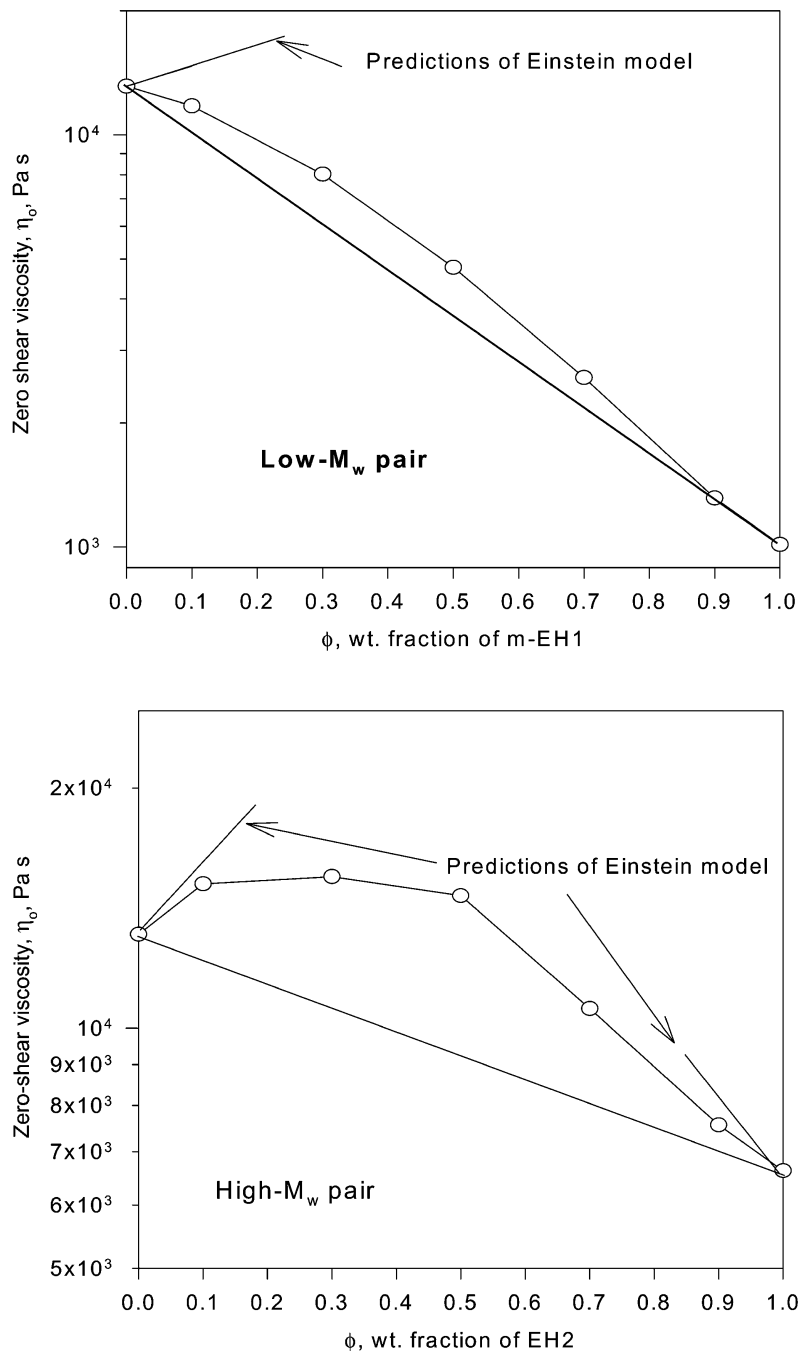


Fig. 4. (a)  $\eta_0(\phi)$  for blends of m-EH1 with LDPE computed from Cross model ( $T_{\text{mix}} = 190^\circ\text{C}$ ,  $T_{\text{test}} = 190^\circ\text{C}$ ,  $\gamma^0 = 15\%$ ). (b)  $\eta_0(\phi)$  for blends of m-EH2 with LDPE computed from Cross model ( $T_{\text{mix}} = 190^\circ\text{C}$ ,  $T_{\text{test}} = 190^\circ\text{C}$ ,  $\gamma^0 = 15$ ). (c)  $\eta'(\phi)$  for blends of m-EH1 with LDPE ( $T_{\text{mix}} = 190^\circ\text{C}$ ,  $T_{\text{test}} = 190^\circ\text{C}$ ,  $\omega = 0.1$  rad/s). (d).  $\eta'(\phi)$  for blends of m-EH2 with LDPE ( $T_{\text{mix}} = 190^\circ\text{C}$ ,  $T_{\text{test}} = 190^\circ\text{C}$ ,  $\omega = 0.1$  rad/s).

ratio of interfacial tension to the droplet radius ( $\alpha/R$ ) from Scholz et al. [35] model. The value of ( $\alpha/R$ ) was calculated as  $\sim 900$  N/m<sup>2</sup>. However, other rheological models that can describe the whole frequency range are now available.

Palierne [44] developed a general expression for the complex shear modulus of an emulsion of viscoelastic fluids

under small-amplitude dynamic shear. For an emulsion of two viscoelastic phases with a uniform particle size and constant interfacial tension, the complex modulus of a blend,  $G_b^*(\omega)$ , is given by

$$G_b^*(\omega) = G_m^* \frac{1 + 3\phi H(\omega)}{1 - 2\phi H(\omega)} \quad (3)$$

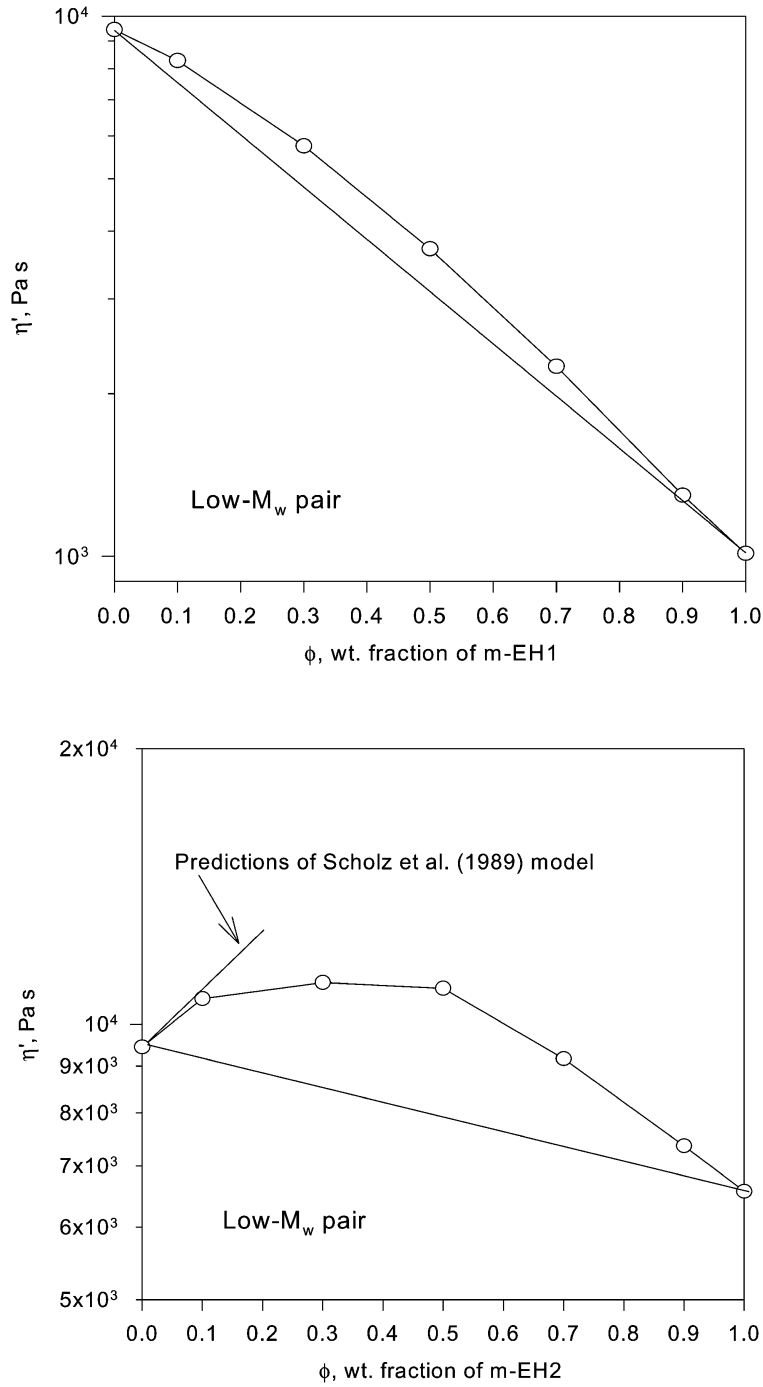


Fig. 4 (continued)

where

$$H(\omega) = \frac{4(\alpha/R)[2G_m^*(\omega) + 5G_d^*(\omega)] - [G_m^*(\omega) - G_d^*(\omega)] \times [16G_m^*(\omega) + 19G_d^*(\omega)]}{40(\alpha/R)[G_m^*(\omega) + G_d^*(\omega)] + [3G_m^*(\omega) + 2G_d^*(\omega)] \times [16G_m^*(\omega) + 19G_d^*(\omega)]} \quad (4)$$

Expressions for  $G'$  and  $G''$  are given elsewhere [45]. Recently, Bousmina [46] extended Kerner's model for modulus of composite solid elastic media [47] to an emulsion of viscoelastic liquid phases with interfacial tension undergoing deformations of small amplitude. Bousmina obtained the

following expression for  $G_b^*(\omega)$

$$G_b^* = G_m^* \frac{2(G_d^* + \alpha/R) + 3G_m^* + 3\phi(G_d^* + \alpha/R - G_m^*)}{2(G_d^* + \alpha/R) + 3G_m^* - 2\phi(G_d^* + \alpha/R - G_m^*)} \quad (5)$$

and showed that his model (Bousmina model) gave

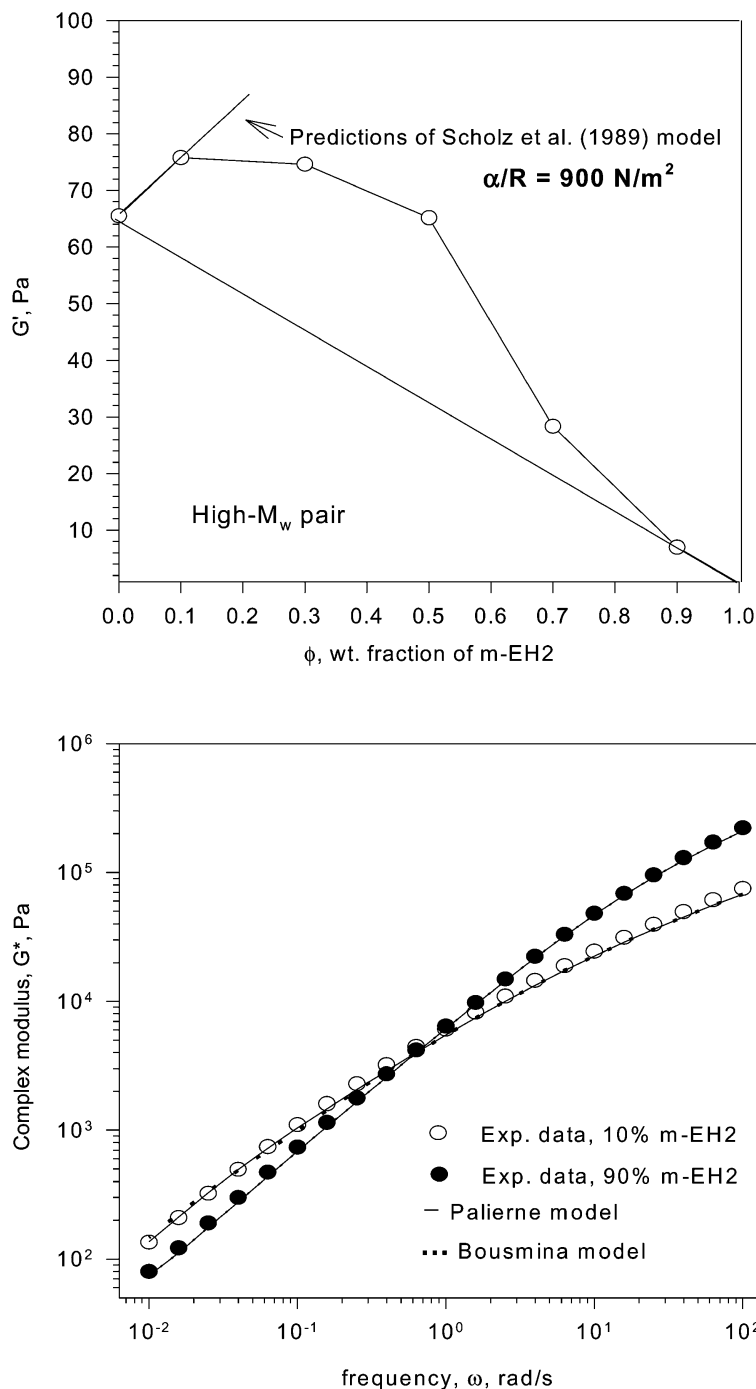


Fig. 5. (a)  $G'(\phi)$  for blends of m-EH2 with LDPE ( $T_{\text{mix}} = 190 \text{ }^\circ\text{C}$ ,  $T_{\text{test}} = 190 \text{ }^\circ\text{C}$ ,  $\gamma^0 = 15\%$ ,  $\omega = 0.1 \text{ rad/s}$ ). (b) Predictions of Palierne and Bousmina models for 10% m-EH2 blend with LDPE ( $T_{\text{mix}} = 190 \text{ }^\circ\text{C}$ ,  $T_{\text{test}} = 190 \text{ }^\circ\text{C}$ ,  $\gamma^0 = 15\%$ ).

predictions similar to those of the Palierne model. Expressions for  $G'(\omega)$  and  $G''(\omega)$  for Bousmina model were published by Hussein and Williams [14].

In the high- $\omega$  non-Newtonian regime, both Palierne and Bousmina models require knowledge of the ratio  $\alpha/R$ ; yet, this is difficult to obtain for polyethylenes. One way of estimating  $\alpha/R$  is to extract that ratio from the low- $\omega$   $G'(\omega)$  data using Eq. 2 (Scholz et al. model [35]) and assume that it stays constant in the high- $\omega$  regime. The above value of  $\alpha/R$

was used for fitting the whole  $G^*(\omega)$  data to Palierne and Bousmina emulsion models as discussed below.

Predictions of both Palierne and Bousmina models for the high- $M_w$  pair were given in Fig. 5(b) for the 10 and the 90% blends. The solid lines represent Palierne model, while the dotted lines are for the Bousmina model. The 90% blend of the high- $M_w$  pair was taken as an example of the likely miscible regime and hence a value of  $\alpha/R = 0$  was used to fit the data. For the 10% blend, Palierne and Bousmina

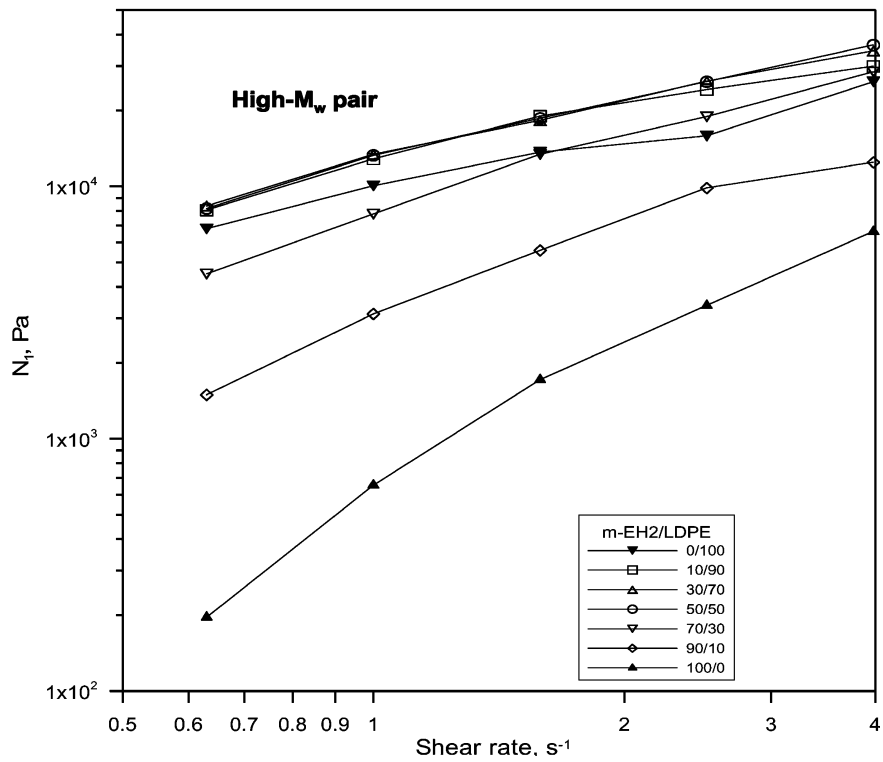
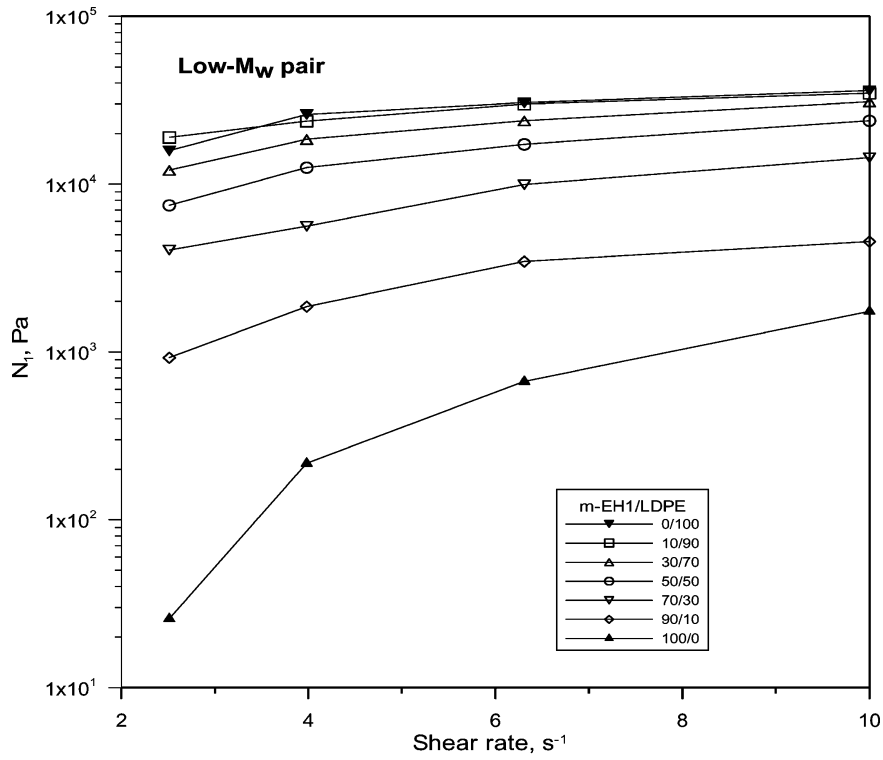


Fig. 6. (a)  $N_1(\dot{\gamma})$  for blends of m-EH1 with LDPE ( $T_{\text{mix}} = 190\text{ }^\circ\text{C}$ ,  $T_{\text{test}} = 190\text{ }^\circ\text{C}$ ,  $t_{\text{bm}} = 200\text{ s}$ ,  $t_{\text{t}} = 30\text{ s}$ ). (b)  $N_1(\dot{\gamma})$  for blends of m-EH2 with LDPE ( $T_{\text{mix}} = 190\text{ }^\circ\text{C}$ ,  $T_{\text{test}} = 190\text{ }^\circ\text{C}$ ,  $t_{\text{bm}} = 200\text{ s}$ ,  $t_{\text{t}} = 30\text{ s}$ ). (c)  $\psi_1(\phi)$  for blends of m-EH2 with LDPE ( $T_{\text{mix}} = 190\text{ }^\circ\text{C}$ ,  $T_{\text{test}} = 190\text{ }^\circ\text{C}$ ,  $\dot{\gamma} = 0.63\text{ s}^{-1}$ ).

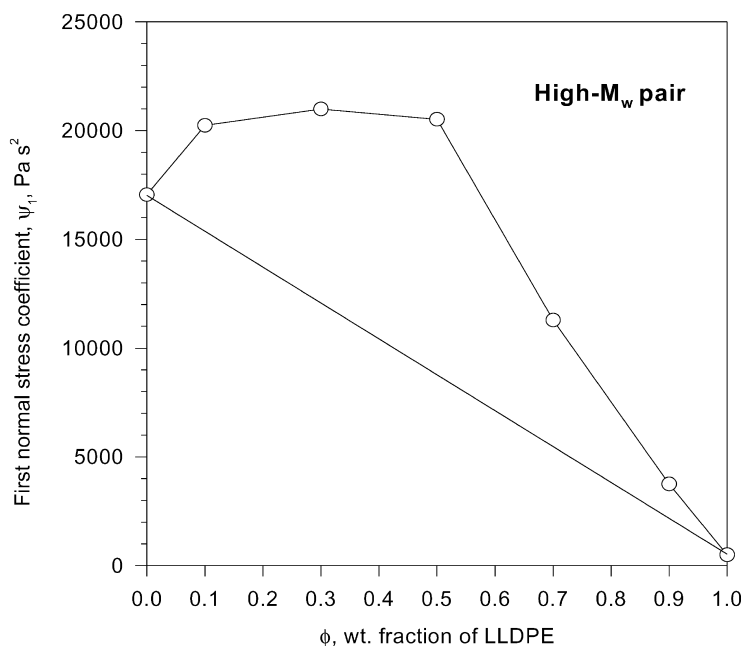


Fig. 6 (continued)

model gave almost the same predictions for  $\alpha/R = 900 \text{ N/m}^2$ . Experimental data and the predictions of both models showed excellent agreement. Also, agreement was obtained between experimental data of  $G^*(\omega)$  for the low- $M_w$  pair and model predictions for the 10% and the 90% blend of the low- $M_w$  pair with LDPE for  $\alpha/R = 0$  (results were not shown here).

All of these predictions suggest the presence of an interface in the LDPE-rich blends and its weakness or absence in the LLDPE-rich blends of the high- $M_w$  pair. For the Low- $M_w$  pair, all models suggest a weak interface, if any, and hence a high degree of miscibility. The value of  $\alpha/R$  obtained for the LDPE-rich blends of the high- $M_w$  pair was comparable with similar values reported for compatibilized polymer blends [48]. If the droplet phase has a size of  $R \cong 1 \mu\text{m}$ , then the order of magnitude of  $\alpha$  is  $\sim 1 \text{ mN/m}$  (1 dyn/cm). Although this value is low; however, it could be due to the chemical similarity of polyethylenes phases.

Thus, the different dynamic shear measurements, discussed so far, suggest the high degree of miscibility of the low- $M_w$  pair. For the high- $M_w$  blend of m-LLDPE with LDPE, high degree of miscibility is likely to occur in the m-LLDPE-rich blends ( $\phi \geq 70\%$  m-LLDPE); and immiscibility is likely to be observed for the 50/50 and LDPE-rich blends ( $\phi \geq 50\%$  LDPE). Einstein, Scholz et al., Palierne and Bousmina models can predict the immiscibility of the blends.

Moreover, steady shear measurements were performed on all blends of m-EH1 and m-EH2 with LDPE using a cone-and-plate geometry. Results of  $N_1(\dot{\gamma})$  for the low- $M_w$  and the high- $M_w$  pairs were displayed in Fig. 6(a) and (b), respectively. Data were shown for the low- $M_w$  pair in the range  $\dot{\gamma} = 2\text{--}10 \text{ s}^{-1}$ , and for the high- $M_w$  pair for  $\dot{\gamma} =$

$0.6\text{--}4 \text{ s}^{-1}$ . For the determination of the morphology of the blend, low- $\dot{\gamma}$  is preferred; however, for the low- $M_w$  pair the choice of the low range was limited by the sensitivity of the rheometer. Results obtained for the low- $M_w$  pair (Fig. 6(a)) show that  $N_1(\dot{\gamma})$  for all blends was bounded by the  $N_1(\dot{\gamma})$  for the pure resins and it increased in proportion to the increase of the more elastic component, the LDPE. Here, the steady-shear data of  $N_1(\dot{\gamma})$  suggests the high degree of miscibility of low- $M_w$  pair and support the above results from dynamic shear measurements.

However,  $N_1(\dot{\gamma})$  data for blends of the high- $M_w$  pair with LDPE were different. In the low- $\dot{\gamma}$  range (sensitive to morphology),  $N_1(\dot{\gamma})$  for the 70 and 90% blend of m-EH2 were found to lie between the  $N_1(\dot{\gamma})$  values for the pure polymers. The 50/50 and the LDPE-rich blends showed  $N_1$  values that were higher than LDPE, the more elastic component. The increase in the elasticity of these blends is a clear indication of a multiphase morphology and is likely a result of the interfacial tension. The steady-shear rheology of blends of m-EH2 with LDPE suggests the immiscibility of the 50/50 and LDPE-rich blends of the high- $M_w$  pair with LDPE; the miscibility of m-LLDPE-rich blends. The first normal stress coefficient,  $\psi_1(\phi)$ , for  $\dot{\gamma} = 0.63$  was plotted in Fig. 6(c). Results were similar to  $G'(\phi)$  data obtained for the same blend at constant  $\omega$  as shown earlier in Fig. 5(a) above.

Once more, another steady-shear test was performed. This time stress relaxations of blends were explored. The relaxation experiment followed a period of 500 s of steady shearing at  $1 \text{ s}^{-1}$ . The test was carried out on all blends of the high and low- $M_w$  pairs as well as the pure resins. Similarly, relaxations of the low- $M_w$  pair given in Fig. 7(a) followed the same pattern of the  $N_1(\dot{\gamma})$  shown in Fig. 6(a). The initial value of  $N_1(t)$  increased in proportion to the

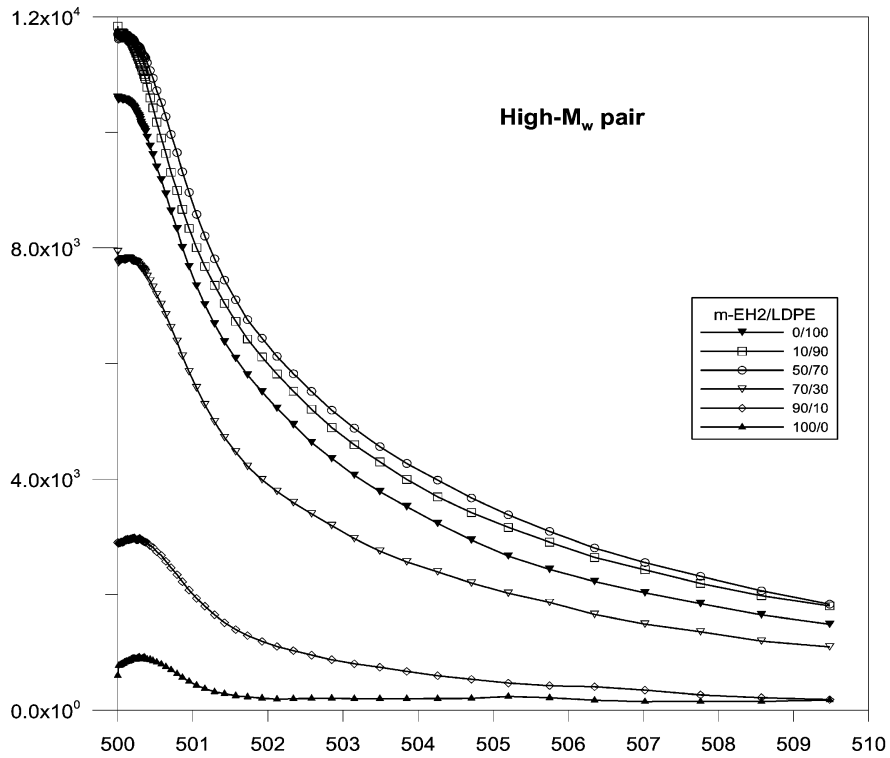
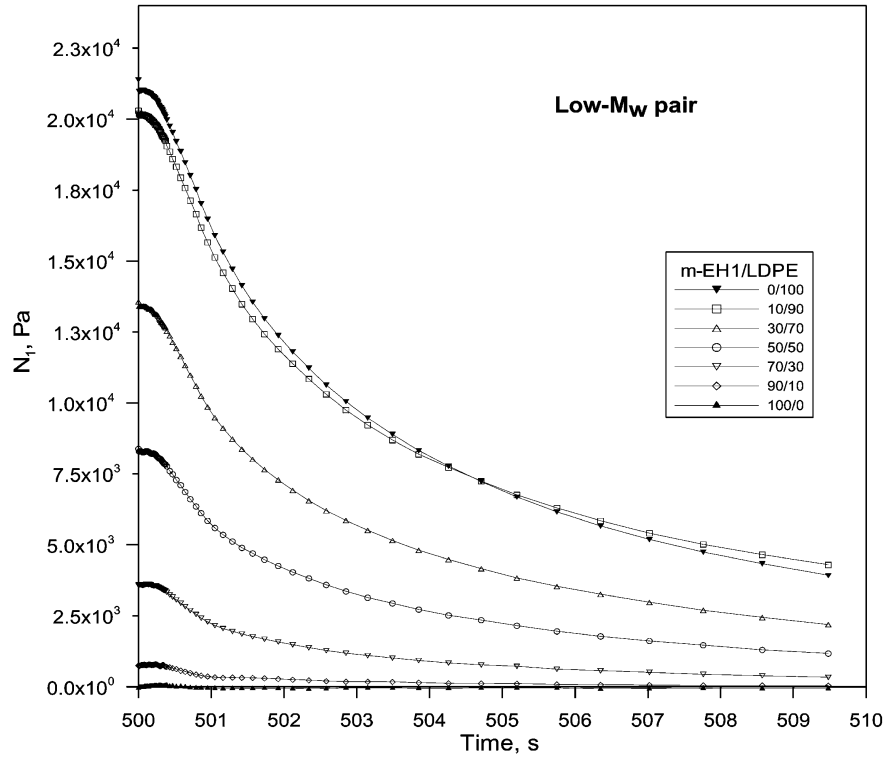


Fig. 7. (a)  $N_1(t)$  relaxations for blends of m-EH1 with LDPE ( $T_{\text{mix}} = 190\text{ }^\circ\text{C}$ ,  $T_{\text{test}} = 190\text{ }^\circ\text{C}$ ,  $\dot{\gamma} = 1.0\text{ s}^{-1}$  for 500 s). (b)  $N_1(t)$  relaxations for blends of m-EH2 with LDPE ( $T_{\text{mix}} = 190\text{ }^\circ\text{C}$ ,  $T_{\text{test}} = 190\text{ }^\circ\text{C}$ ,  $\dot{\gamma} = 1.0\text{ s}^{-1}$  for 500 s).

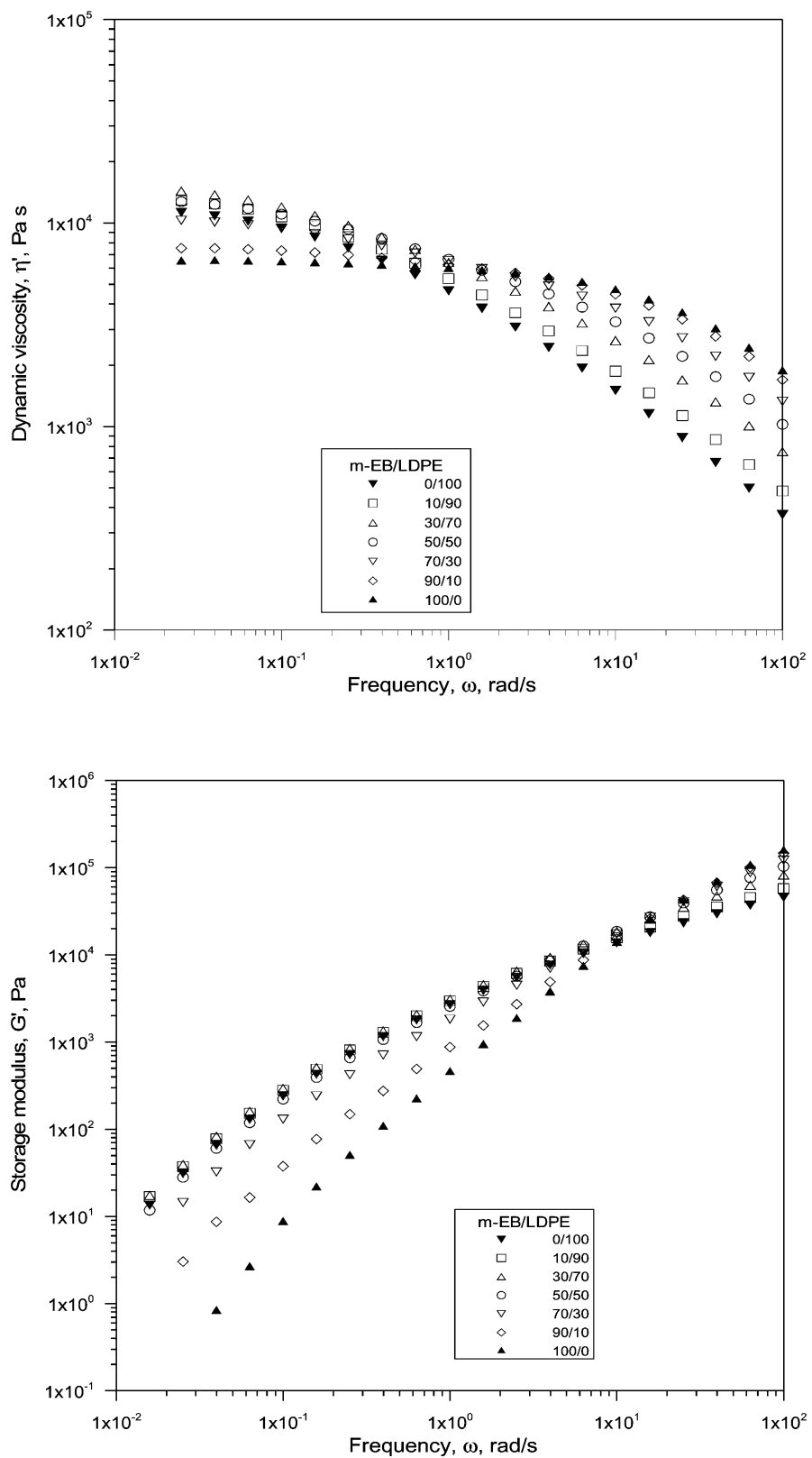


Fig. 8. (a)  $\eta'(\omega)$  for blends of m-EB with LDPE ( $T_{\text{mix}} = 190^\circ\text{C}$ ,  $T_{\text{test}} = 190^\circ\text{C}$ ,  $\gamma^0 = 15\%$ ,  $\omega = 0.1$  rad/s). (b)  $G'(\omega)$  for blends of m-EB with LDPE ( $T_{\text{mix}} = 190^\circ\text{C}$ ,  $T_{\text{test}} = 190^\circ\text{C}$ ,  $\gamma^0 = 15\%$ ,  $\omega = 0.1$  rad/s).

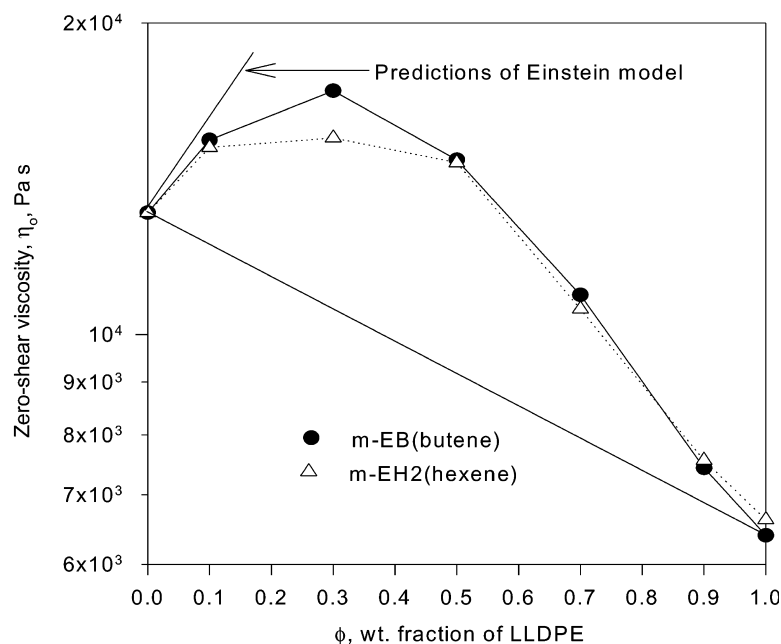


Fig. 9.  $\eta_0(\phi)$  for blends of m-EH2 and m-EB with LDPE computed from Cross model ( $T_{\text{mix}} = 190^\circ\text{C}$ ,  $T_{\text{test}} = 190^\circ\text{C}$ ,  $\gamma^0 = 15\%$ ).

fraction of the LDPE. At shorter times ( $t < 4$  s), relaxations were faster for the low- $M_w$  component (m-EH1) and it slowed down with increasing fraction of LDPE. These relaxations suggest the mingling of the two polymers and the increase in the average  $M_w$  of the blend has produced an equivalent increase in the relaxation. It should be noted that the relaxation of the 10% blend of the low- $M_w$  component was almost the same as that of the LDPE. The result may suggest partial immiscibility of this pair. The same observation can be drawn from  $N_1(\dot{\gamma})$  data for the 10% blend shown in Fig. 6(a) at low- $\dot{\gamma}$  as well as from the weak PDB of  $\eta_0(\phi)$  shown in Fig. 4(a). However, the deviation from predictions of emulsion was large and hence partial miscibility was suggested. Previous dynamic tests did not show this behavior explicitly.

On the other hand, the  $N_1(t)$  curves for the high- $M_w$  pair, displayed in Fig. 7(b), followed a pattern similar to that of  $N_1(\dot{\gamma})$  given in Fig. 6(b). Here, the initial values of  $N_1$  for the 50/50 and LDPE-rich blends were higher than that of the highest molecular weight component (LDPE). This result supports the previous dynamic and steady-shear data in suggesting the presence of emulsion system even after a steady shearing of 500 s. The presence of an interface is responsible for the increase in  $N_1$  beyond that of pure components. Likewise, at short times the curves were very distinct and they provided clear indications of immiscibility of the m-LDPE-rich blends with LDPE. The m-LLDPE-rich blends were deemed partially miscible with a high degree of miscibility at high  $\phi$ . Or, the miscibility of the hexene-based m-LLDPE with LDPE is non-symmetric with respect to composition.

Most of the previous rheological investigations of multiphase systems have concentrated on dynamic-shear

rheology, but it seems that the steady-shear rheology, especially the relaxation measurements were very informative and they take shorter times. Further analysis of the relaxation data and fittings to models will be addressed elsewhere [49].

The different methods of presenting the dynamic and steady-shear data suggest a role for  $M_w$  in the miscibility of m-LLDPE/LDPE systems. The low- $M_w$  pair is believed to be almost miscible. However, the high- $M_w$  pair is immiscible or partially miscible over the whole composition range. The 50/50 and LDPE-rich blends of the high- $M_w$  pair are likely immiscible; and the LLDPE-rich blends are partially miscible with a high degree of miscibility at  $\phi \geq 0.7$ . Hence, in blends of high- $M_w$  component m-EH2 and LDPE a 10% m-EH2 blend is likely to be immiscible while that of 90% m-EH2 is likely miscible. The immiscibility of the blends could be predicted by Einstein, Scholz et al., Palierne and Bousmina models in the sense that they predict  $G^*(\omega)$  accurately based on the assumption of 2-phase behavior.

In general, the results of the current study on the m-LLDPE high- $M_w$  pair were similar to the previous findings of Utracki and Schlund [10] on butene ZN-LLDPE blends with LDPE. PDB was observed in both cases. However, the plot of  $\eta_0(\phi)$  was almost symmetric for the case of ZN-LLDPE systems (Fig. 12 of Ref. [10]), while non-symmetry was observed in this study (Figs. 4(b) and 9) that used m-LLDPEs. The weak miscibility of ZN-LLDPE-rich blends [10] in comparison to the m-LLDPE-rich blends (current study) might be due to the presence of the linear chains in ZN-LLDPE. It should be noted that each ZN-LLDPE is by itself a 'unique' soup of molecular structures, which makes this comparison very difficult. The current findings with

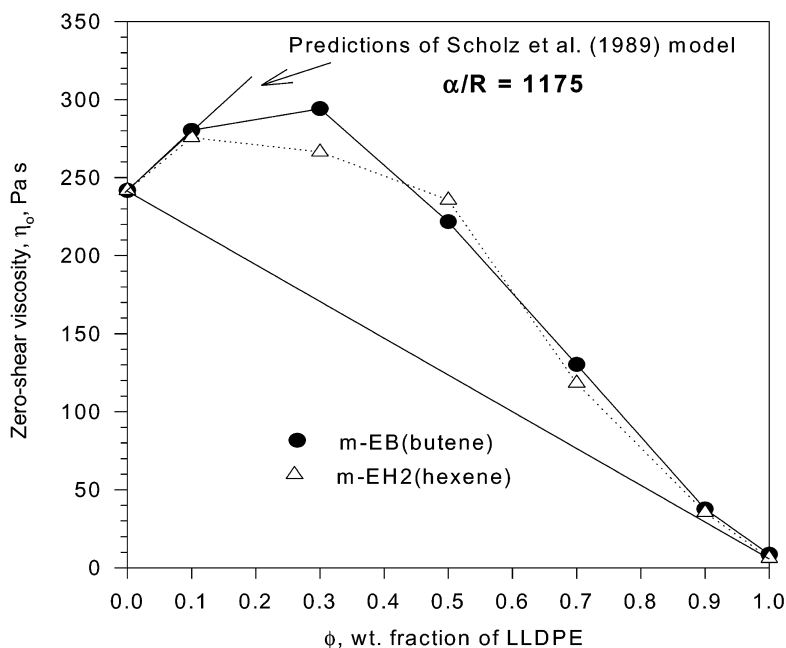


Fig. 10.  $G'(\phi)$  for blends of m-EH2 and m-EB with LDPE computed from Cross model ( $T_{\text{mix}} = 190^\circ\text{C}$ ,  $T_{\text{test}} = 190^\circ\text{C}$ ,  $\gamma^0 = 15\%$ ,  $\omega = 0.1$  rad/s).

regard to the effect of  $M_w$  on miscibility of m-LLDPE/LDPE blends are similar to the observations of Tanem and Stori [4] on m-LLDPE blends with linear polyethylene.

### 3.2. Influence of comonomer type

To study the influence of the comonomer type another blend of a metallocene butene LLDPE (m-EB) with LDPE was investigated. The m-EB resin was chosen to have about the same  $M_w$  and density ( $M_w = 110\text{k}$ ;  $\rho = 0.900$  g/cm<sup>3</sup>) as

the corresponding hexene m-LLDPE ( $M_w = 108\text{k}$ ;  $\rho = 0.900$  g/cm<sup>3</sup>). The m-EB resin was blended with the same LDPE in the presence of additional 1000 ppm extra amount of AO. The blending and testing conditions were the same as mentioned earlier. Dynamic, steady shear and transient measurements were performed on the butene-based blends. Plots of  $\eta'(\omega)$  and  $G'(\omega)$  for blends of m-EB with LDPE were shown in Fig. 8(a) and (b), respectively. Results of  $\eta'(\omega)$  and  $G'(\omega)$  were almost identical to those obtained for the m-EH2 pair and given in Fig. 3(a) and (b).

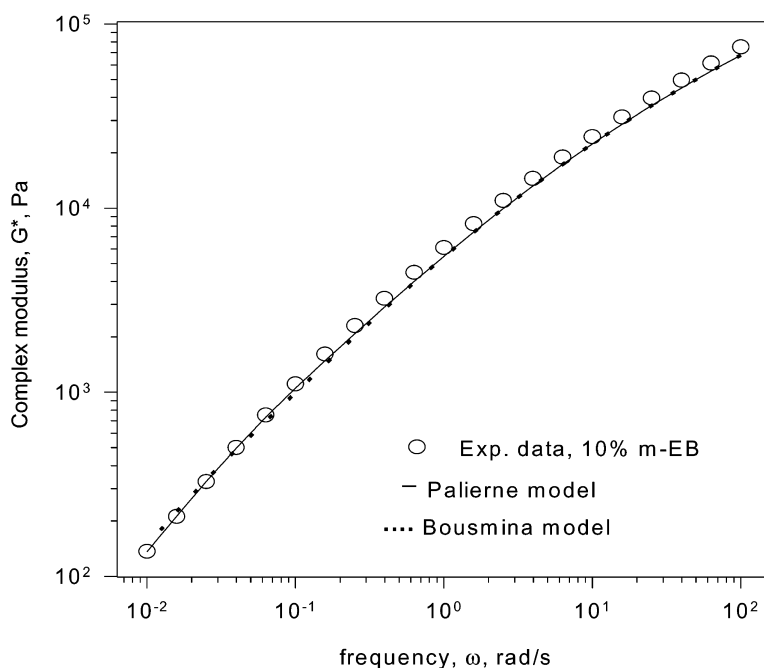


Fig. 11. Predictions of Palierne and Bousmina models for the 10% m-EB blend with LDPE ( $T_{\text{mix}} = 190^\circ\text{C}$ ,  $T_{\text{test}} = 190^\circ\text{C}$ ,  $\gamma^0 = 15\%$ ).

This is a direct consequence of matching the  $M_w$  (sensitive to viscosity) and density (sensitive to branching and hence elasticity). Here, the hexene-based blend showed a Newtonian plateau over more than a decade. Also, the metallocene resin was the component of the lowest viscosity and elasticity over the low- $\omega$  range (0.01–0.1 rad/s). In the low- $\omega$  range, blends with 50, 30, and 10% m-EB showed both  $\eta'$  and  $G'$  that were higher than those of LDPE. Both  $\eta'$  and  $G'$  of LDPE have increased as a result of its blending with a low viscosity (and elasticity) component. This observation can only be explained by emulsion rheology. The data shown in Fig. 8(a) and (b) suggest the immiscibility of the 50/50 and LDPE-rich blends and the miscibility of the 90% m-EB blend. The 70% m-EB blend is believed to be partially miscible as will be discussed below.

The  $\eta'(\omega)$  data for blends of m-EB with LDPE were fitted by ARES Orchestrator software to Cross the model. Computed  $\eta_0$  was obtained from the fitting and plotted in Fig. 9. The plot showed PDB for the LDPE-rich and the 50/50 blends, while  $\eta_0$  almost followed the log-additivity for the 90% m-EB blend.

The  $\eta_0(\phi)$  data for the butene-based and the hexene-based blends were almost identical and the deductions regarding the miscibility/immiscibility of the butene-based blend were identical to those of the hexene-based blend discussed earlier. However, here we concentrate on the effect of increasing the branch length from butene to hexene. It is evident that increasing the branch length from butene to hexene has little or no effect on the miscibility of m-LLDPE/LDPE systems.

Also, similar conclusions can be withdrawn from the comparison of the  $G'(\phi)$  for the butene-based and hexene-based blends (see Fig. 10). Predictions of Einstein model (Newtonian viscosities were used) given in Fig. 8(a) and Scholz et al. model [35] shown in Fig. 8(b) support the above conclusions regarding the miscibility of the 50/50 and the LDPE-rich blends and the high degree of miscibility of the 90% blend for m-EB and m-EH2 blends. To determine the degree of immiscibility of the 70% blend both Einstein and Scholz models were used to predict  $\eta_0$ ,  $\eta'$  and  $G'$ . Both models predicted values that were higher than the experimental results; hence, the 70% blend of m-EH2 and m-EB with LDPE was deemed to be partially miscible. Hence, strong immiscibility was observed when a small amount of m-LLDPE was added to LDPE (LDPE-rich blends), while miscibility was achieved when a small amount of LDPE was added to m-LLDPE (m-LLDPE rich blends). Or, the effect of composition on the miscibility of butene-based m-LLDPE blends with LDPE is non-symmetric.

On the other hand, predictions of Palierne and Bousmina models for the butene-based blends were displayed in Fig. 11 for the 10% m-EB blend with LDPE. The solid lines represent the predictions of  $G^*(\omega)$  for Palierne model computed using Eqs. 3 and 4 above. The dotted lines correspond to the estimations of Bousmina model calculated

using Eq. 5. The 90% blend of the butene-based blend was taken as an example of the miscible regime and hence a value of  $\alpha/R = 0$  was used to fit the data. Results (not shown here) were in excellent agreement with experimental data similar to what was shown earlier in Fig. 5(b). For the 10% EB blend with LDPE, both Palierne and Bousmina models gave almost the same predictions for  $\alpha/R = 1175 \text{ N/m}^2$ . Excellent agreement between experimental data and model predictions was observed. This value of  $\alpha/R$  was of the same order of magnitude as that obtained for the hexene-based blend, which suggest little influence for the increase of branch length from butene to hexene.

The above results suggest the immiscibility of the 10, 30, and 50% m-EH1 and m-EB blends with LDPE; the partial miscibility of the 70% blend and the high degree of miscibility of the 90% blend. Hence, blends of the high- $M_w$  pair with LDPE were likely immiscible for the 50/50 and the LDPE-rich blends and likely partially miscible for the m-LLDPE rich blends.

The different rheological measurements and data treatment techniques have supported the high degree of miscibility of the 90% m-EH1 and m-EB blends with LDPE. For the 50/50 and LDPE-rich blends, both butene-based and hexene-based blends of m-LLDPE with LDPE were suggested to be immiscible. Overall, the effect of composition on the miscibility of the shortly branched m-LLDPE and LDPE systems (butene or hexene-based) was found to be non-symmetric.

The present study suggests no influence for comonomer type (butene vs. hexene) on the miscibility of m-LLDPE blends with LDPE. These results were similar to the previous observations on blends of linear and LLDPE systems obtained from different techniques [2,4,25,50]. However, others have observed reduced immiscibility in the case of blends of octene LLDPE and linear polyethylene [50,51].

At this stage we would like to provide tentative explanations for immiscibility of polyethylenes. The m-EH2 and the LDPE used in this study have almost the same average  $M_w$  and density (Table 1), suggesting that the two components have equivalent molecular volumes. However, the above results show that adding a small amount of the metallocene LLDPE to the LDPE is more likely to cause immiscibility than the addition of a small amount of LDPE to LLDPE (Figs. 4(b) and 5(a)). These experimental findings are in agreement with theoretical predictions of Ref. [53]. They showed that the presence of compositional non-symmetry in polyolefin blends even if the two components have equivalent overall molecular volumes. Therefore, adding a small amount of a highly branched component to a lightly branched melt is more likely to cause liquid-liquid phase separation than vice versa [52].

This non-symmetric influence of  $M_w$  on the miscibility of high- $M_w$  m-LLDPE/LDPE blends shown above, suggests an unexpectedly strong influence of molecular structure, possibly more so than molecular weight, on the miscibility

of polyethylenes. This seems consistent with theoretical findings [53,54] that acknowledge the importance of the *conformational* and *architectural* ‘mismatch’ between components of polyolefin blends on their miscibility. The evidences of molecular order in melts of linear polyethylene [55] suggests different conformations for different types of PEs depending on type, content and distribution of branching as supported by the recent molecular dynamics simulations [56].

#### 4. Conclusions

Several rheological measurements and data-treatment approaches were used in this study. First, plots of  $\eta_0(\phi)$ ,  $\eta'(\omega)$ ,  $\eta'(\phi)|_{\omega=\text{const}}$ ,  $G'(\omega)$ ,  $G'(\phi)|_{\omega=\text{const}}$ ,  $G^*(\omega)$ ,  $N_1(\dot{\gamma})$ ,  $N_1(t)$  were shown to be helpful. These techniques and approaches made it possible to identify the miscibility/immiscibility of the high- $M_w$  blends. Second, the three-parameter Cross model was used to model  $\eta'(\omega)$  data, allowing the assessment of miscibility through  $\eta_0(\phi)$ . Third, steady shear measurements of  $N_1(\dot{\gamma})$  and  $N_1(t)$  were found to be very enlightening on miscibility, especially  $N_1(t)$ .

In conclusion, the effects of molecular weight and branch type on the miscibility of LLDPE/LDPE blends were investigated. The following is a summary of the previous observations as suggested by the different methods of data analysis:

The  $M_w$  of the shortly branched m-LLDPE has influenced its miscibility with LDPE. Blends of low- $M_w$  m-LLDPE (hexene) and LDPE were almost *miscible* in almost the whole composition range.

The miscibility of the hexene-based m-LLDPE with LDPE is non-symmetric with respect to composition. Addition of a small amount of the hexene m-LLDPE to LDPE is more likely to cause immiscibility than the addition of a small amount of LDPE to m-LLDPE.

Blends of high- $M_w$  m-LLDPE (hexene) and LDPE mixed at 190 °C were *partially miscible*. *Immiscibility* is likely to occur around the 50/50 composition and in the LDPE-rich blends. Blends were either partially miscible or likely *miscible* in the LLDPE-rich range.

The immiscibility of the blends leads to increase in  $\eta_0(\phi)$ ,  $\eta'(\phi)$ ,  $G'(\phi)$  and  $G^*(\omega)$  that can be explained by *emulsion* models (e.g. Einstein and Scholz et al dilute emulsion models; Palierne and Bousmina model).

The ratio of interfacial tension to droplet radius ( $\alpha/R$ ) was found to be in the order of  $10^3$  N/m<sup>2</sup> as computed from rheological models. The value of  $\alpha/R$  is consistent with an interface between chemically similar polyethylene.

The ‘mismatch’ in the molecular *conformation* of m-LLDPE and LDPE is likely responsible for the immiscibility.

Matching the density and  $M_w$  of the hexene-based and the butene based metallocene LLDPE resulted in almost identical rheology. Increasing the branch length from butene to hexene in m-LLDPE has no effect on its miscibility with LDPE, which is similar to previous observations on blends of linear polyethylene with LLDPE.

#### Acknowledgements

Financial support for this project was provided by KFUPM under project # CHE/Rheology/223. Authors are thankful to Professor Abdullah A. Shaikh, former chairman of the Chemical Engineering Department for his support and help in establishing the Polymer Research Lab at the Chemical Engineering Department. We are thankful to Mr Willy Leysen of ExxonMobil, Belgium for providing polyethylene samples. We are also grateful to Dr Naseem Akhtar for his help with the GPC characterization.

#### References

- [1] Crist B, Hill MJ. J Polym Sci Polym Phys 1997;35:2329.
- [2] Hill MJ, Barham PJ. Polymer 1997;38:5595.
- [3] Alamo RG, Londono JD, Mandelkern L, Stehling FC, Wignall GD. Macromolecules 1994;27:2864.
- [4] Tanem BS, Stori A. Polymer 2001;42:4309.
- [5] Tanem BS, Stori A. Polymer 2001;42:5689.
- [6] Muñoz-Escalona A, Lafuente P, Vega JF, Muñoz ME, Santamaria A. Polymer 1997;38(3):589.
- [7] Utracki LA. Polymer alloys and blends: thermodynamics and rheology. NY: Hanser; 1989.
- [8] Utracki LA. In: Utracki LA, Weiss RA, editors. Melt flow of polyethylene blends in multiphase polymers: blends and ionomers. ACS symposium series. Washington, DC: ACS; 1989.
- [9] Hill MJ, Barham PJ. Polymer 1995;36:1523.
- [10] Utracki LA, Schlund B. Polym Engng Sci 1987;27(20):1512.
- [11] Datta NK, Birley AW. Plast Rubber Process Appl 1983;3(3):237.
- [12] Muller AJ, Balsamo V. Adv Polym Blends Alloys Technol 1994;5(1): 21.
- [13] Lee HS, Denn MM. Polym Engng Sci 2000;40:1132.
- [14] Hussein IA, Williams MC. J Polym Engng Sci 2001;41(4):696.
- [15] Xu J, Xu X, Chen L, Feng L, Chen W. Polymer 2001;42:3867.
- [16] Usami T, Gotoh Y, Takayama S. Macromolecules 1986;19:2722.
- [17] Freed KF, Dudowicz J. Macromolecules 1996;29:625.
- [18] Zhang M, Lynch DT, Wanke SE. Polymer 2001;42:3067.
- [19] Hill MJ, Puig CC. Polymer 1997;38:1921.
- [20] Munstedt H, Kurzbeck S, Egersdorfer L. Rheol Acta 1998;37:21.
- [21] Gabriel C, Kaschta J, Munstedt H. Rheol Acta 1998;37:7.
- [22] Wardhaugh LT, Williams MC. Polym Engng Sci 1995;35(1):18.
- [23] Hill MJ, Barham PJ, Keller A. Polymer 1992;33:2530.
- [24] Hill MJ. Polymer 1994;35:1991.
- [25] Hill MJ, Barham PJ. Polymer 1997;38:5595.
- [26] Reichart GC, Graessley WW, Register RA, Lohse DJ. Macromolecules 1998;31:7886.
- [27] Plochocki AP. In: Paul DR, Newman S, editors. Polyolefin blends: rheology, melt mixing, and applications in polymer blends, vol. 2. New York: Academic Press; 1978.
- [28] Chuang CI, Han CD. J Appl Polym Sci 1994;29:2205.
- [29] Larson RG. Rheol Acta 1992;31:497.

- [30] Minale M, Moldenaers P, Mewis J. *Macromolecules* 1997;30:5470.
- [31] Utracki LA. *Polym Engng Sci* 1988;28(21):1401.
- [32] Taylor GI. *Proc R Soc* 1932;A138:41.
- [33] Oldroyd JG. *Proc R Soc* 1953;A128:122.
- [34] Choi SJ, Schowalter WR. *Phys Fluids* 1997;18(4):420.
- [35] Scholz P, Froelich D, Muller R. *J Rheol* 1989;33(3):481.
- [36] Gramespacher H, Meissner J. *J Rheol* 1992;36(6):1127.
- [37] Fujiyama M, Kawasaki Y. *J Appl Polym Sci* 1991;42:481.
- [38] Graebing D, Muller R, Paliarne JF. *Macromolecules* 1993;26:320.
- [39] Aiji A, Choplin L. *Macromolecules* 1991;24:5221.
- [40] Martinez CB, Williams MC. *J Rheol* 1980;24(4):421.
- [41] Hussein IA, Ho K, Goyal SK, Karbaszewski K, Williams MC. *Polym Degrad Stab* 2000;68:381.
- [42] Einstein A. *Ann Phys* 1906;19:289. 1911;34:591.
- [43] Oene V. In: Paul DR, Newman S, editors. *Rheology of polymer blends and dispersions in polymer blends*, vol. 1. New York: Academic Press; 1978.
- [44] Paliarne JF. *Rheol Acta* 1990;29:204. Erratum 1991;30:497.
- [45] Carreau PJ, De Kee DCR, Chhabra RP. *Rheology of polymeric systems: principles and applications*. Munich: Hanser; 1997. p. 338. Chapter 8, p. 338.
- [46] Bousmina M. *Rheol Acta* 1999;38:73.
- [47] Kerner EH. *Proc Phys Soc* 1956;B69:808.
- [48] Brahim B, Ait-Kadi A, Aiji A, Jerome R, Fayt R. *J Rheol* 1991;35:1069.
- [49] Hameed T. *Rheological and Molecular Dynamic simulation study of the miscibility of LDPE and m-LLDPE blends*. MS Thesis. King Fahd University of Petroleum and Minerals, Dhahran, Saudi Arabia, in preparation.
- [50] Hussein IA, Williams MC. Submitted for publication.
- [51] Hill MJ, Barham PJ, van Ruiten J. *Polymer* 1993;34:2975.
- [52] Fredrickson GH, Liu AJ, Bates FS. *Macromolecules* 1994;27:2503.
- [53] Fredrickson GH, Liu AJ. *J Polym Sci, Part B: Polym Phys* 1995;33:1203.
- [54] Bates FS, Fredrickson GH. *Macromolecules* 1994;27:1065.
- [55] Hussein IA, Williams MC. *J Non-Newtonian Fluid Mech* 1999;86(1/2):105–18.
- [56] Abu Sharkh BF, Hussein IA. *Polymer* 2002; in press.